ORGANIC CHEMISTRY FRONTIERS

RESEARCH ARTICLE

View Article Online
View Journal

Published on 16 April 2021. Downloaded by Shaanxi Normal University on 5/27/2021 1:48:51 AM.

Check for updates

Cite this: DOI: 10.1039/d1qo00322d

Mechanistic studies on nickel-catalyzed enantioselective [3 + 2] annulation for γ-butenolide synthesis *via* C–C activation of diarylcyclopropenones†

Dachang Bai, *‡[a,b] Song Liu,‡[c,d] Junyan Chen,[a] Yanjiang Yu,[a] Manman Wang,[a] Junbiao Chang,[a] Yu Lan *[c] and Xingwei Li *[a,e]

Received 4th March 2021,
Accepted 6th April 2021

DOI: 10.1039/d1qo00322d

rsc.li/frontiers-organic

Highly efficient Ni-catalyzed C–C activation of cyclopropenones *en route* to enantioselective [3 + 2] annulation with α-CF_3 enones or 1,2-diones has been realized toward the efficient synthesis of γ-butenolides. Mechanistic aspects such as exceptionally high efficiency, unusual enone carbonyl-participated chemoselectivity, and enantioselective control have been elucidated by an integrated experimental and computational approach. DFT studies revealed a key step of oxidative addition of cyclopropenone to enone-ligated nickel, followed by an unusual *endo*-type 4,1-insertion to give a tethered allyl–Ni(II) intermediate. Stereo-determining C–C reductive elimination of this allyl species affords the [3 + 2] annulation product. Computational studies also suggested that coordination of the olefin unit of enone dramatically decreases the activation barrier of subsequent C–C oxidative addition of cyclopropenone. Moreover, a three-coordinate Ni(0) olefin complex (confirmed by X-ray crystallography) was experimentally and theoretically identified as the resting state of the catalyst.

Introduction

Metal-catalyzed C–C bond activation, which allows facile reconstruction of the framework of organic substrates, has been established as an increasingly attractive strategy for the rapid construction of complex structures in an atom-economical fashion.[1] Compared with C–H bonds, the C–C bond is generally less sterically accessible, and the σ orbital in C–C bonds is also more directional, which leads to a high kinetic barrier during interactions with transition metals. Thus, two strategies have been frequently adopted to address this challenge, namely, use of ring strain and a proximal chelating group.[1,2] Despite increasing reports on C–C bond activation systems, studies on enantioselective transformation through C–C bond activation severely lag behind, even for strained ring systems. In recent years, Dong,[3] Cramer,[4] Murakami,[5] and other groups[6] demonstrated notable breakthroughs in rhodium- and nickel-catalyzed intramolecular insertion of π-bonds into C–C bonds in enantioselective fashions (Scheme 1a), where chelation-assistance and ring strain were collectively employed to enhance both the reactivity and regioselectivity for the efficient synthesis of fused and bridged cycles. However, these π-bonds have been often restricted to carbon–carbon bonds in monofunctional substrates such as alkenes, alkynes, 1,3-dienes, and enones.[1,2]

In contrast to intramolecular systems, intermolecular enantioselective coupling systems have been rarely reported, where the issues of chemo- and regioselectivity may often arise. As a first-row transition metal, nickel(0) plays an appealing role in this challenging area.[7,8] In 2017, Ye and coworkers elegantly reported Ni–Al co-catalyzed enantioselective cycloaddition of cyclopropyl carboxamide with alkyne *via* C–C activation (Scheme 1a).[7] This system development is challenging and requires cooperation of two metals even though the coupling partner (alkyne) seems reactive. In previous studies, the coupling partner to the C–C bond is either intramolecular or mono-functional. Therefore, complication of chemoselectivity will arise if the coupling partner bears multifunctionality

[a]Henan Key Laboratory of Organic Functional Molecule and Drug Innovation, School of Chemistry and Chemical Engineering, Henan Normal University, Xinxiang 453007, China. E-mail: baidachang@htu.edu.cn, lixw@snnu.edu.cn
[b]State Key Laboratory of Organometallic Chemistry, Shanghai Institute of Organic Chemistry, Chinese Academy of Sciences, Shanghai 200032, P R China
[c]School of Chemistry and Chemical Engineering, Chongqing University, Chongqing 400030, China. E-mail: lanyu@cqu.edu.cn
[d]Chongqing Key Laboratory of Environmental Materials and Remediation Technologies, Chongqing University of Arts and Sciences, Chongqing, 402160, P. R. China
[e]School of Chemistry and Chemical Engineering, Shaanxi Normal University (SNNU), Xi'an 710062, China

†Electronic supplementary information (ESI) available. CCDC 2034194, 2034195 and 1962621. For ESI and crystallographic data in CIF or other electronic format see DOI: 10.1039/d1qo00322d

‡These authors contributed equally.

Published on 16 April 2021. Downloaded by Shaanxi Normal University on 5/27/2021 1:48:51 AM.

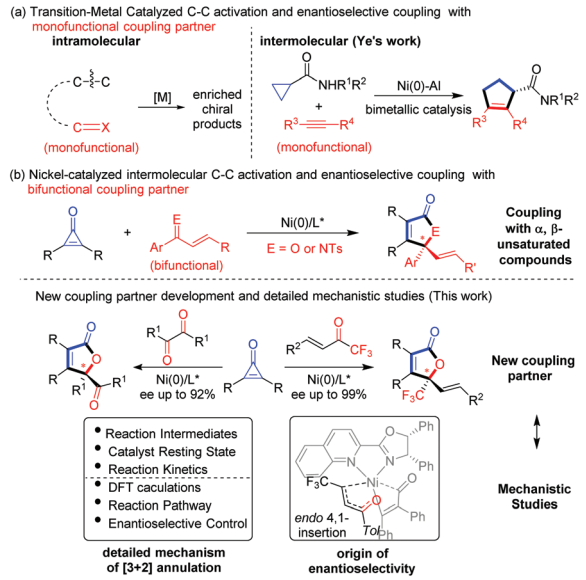

Scheme 1 Nickel-catalyzed C–C activation and enantioselective coupling system. (a) Transition-metal catalyzed C–C activation and enantioselective coupling with a monofunctional coupling partner. (b) Nickel-catalyzed C–C activation and enantioselective coupling with a bifunctional coupling partner.

(Scheme 1a). Very recently, our group briefly reported nickel-catalyzed enantioselective [3 + 2] annulation of cyclopropenones with α,β-unsaturated ketones/imines through C–C activation.[8] The most striking feature of this system is the exclusive C=O insertion. In addition, the reaction enantioselectivity is well controlled, which offers a chemoselective [3 + 2] annulation approach to access enriched γ-alkenyl-butenolides and γ-lactams (Scheme 1b).[9] While this C–C activation system proved to be efficient, the origin of chemoselectivity and enantioselectivity remains big mechanistic puzzles. The rarity of enantioselective C–C activation and the unusual chemoselectivity inspired us to conduct detailed mechanistic studies, which may provide important insights into the future development of enantioselective systems *via* C–C activation. Herein we report the applications of other bifunctional coupling partners for chemoselective γ-butenolide synthesis through nickel-catalyzed C–C bond activation. In addition, mechanistic studies of this system by integration of experimental and computational methods (DFT) revealed an *endo*-type 4,1-insertion transition state of carbonyl from enone into the Ni–acyl bond as the origin of the chemo- and enantioselectivity. This new mechanistic profile provides new insights into the unique high reactivity of the catalytic system and may benefit the future development of other C–C activation systems (Scheme 1b).

Results and discussion

High efficiency

The efficiency of the coupling system that we previously developed was further examined. As shown in Table 1, when the

Table 1 High efficiency of the Ni/**L1** catalyst for the coupling of diphenylcyclopropenone **1a** and enone **2a**[a]

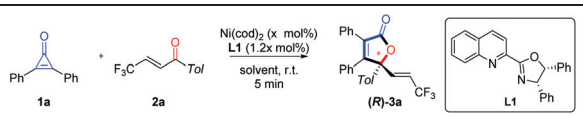

Entry	X	Solvent	Yield (%)	ee (%)	TOF (h^{-1})
1	1.0	Toluene	99	95	1188
2	0.5	Toluene	51	95	1224
3	0.5	MeO^{t}Bu	92	93	2208

[a] Reaction conditions: **1a** (0.2 mmol), enone **2a** (0.2 mmol), Ni(cod)$_2$ and a chiral ligand in a solvent (2.0 mL) under argon for 5 min, isolated yield. The ee was determined by HPLC on a chiral stationary phase.

catalyst loading of Ni/**L1** was reduced to 0.5 mol%, the desired product **3a** was obtained in 51% yield and 95% ee within 5 min (entries 1 and 2). When the solvent was changed to MeO^{t}Bu, the desired product **3a** was obtained in 92% yield and 93% ee, which correspond to a TOF of 2208 h^{-1} (entry 3 and ESI Table 1†). Such catalytic activity is exceptional in enantioselective coupling systems *via* C–C bond activation.

With the highly efficiency in hand (Table 1),[8] we further explored new coupling partners for this reaction system. After detailed studies of the reaction parameters of the coupling of α-CF_3 enone and cyclopropenone **1a** (Table S2 in the ESI†), γ-CF_3-butenolide product **4a** was obtained in a high yield with excellent enantioselectivity.[10] However, other carbonyl compounds such as acetophenone and benzaldehyde failed to undergo the desired reaction. We reasoned that α-dicarbonyl compounds may be more reactive than simple carbonyl compounds.[11] Thus, benzil was applied as a coupling partner in the reaction with **1a** with Ni(cod)$_2$/Pybox **L1** as the catalyst (Table 2). Initial studies showed that the desired product **5a** was obtained only in a low yield with moderate enantioselectivity in toluene at 60 °C (Table 2, entry 1). Further screening of the solvent failed to give better results (entries 1–8). Screening of the ligand revealed that the oxazoline ring with *cis* vicinal diphenyl substituents gave higher enantioselectivity (entries 9–11). Inspired by these results, several new Pybox ligand bearing bulk substituents at the C-6 position were synthesized. To our delight, ligand **L6** with a diphenylmethyl group at the C-6 position gave much better results (entries 12–14). Decreasing the temperature to 0 °C resulted in a good yield and excellent enantioselectivity (76% yield, 90% ee). Further decreasing the temperature to −20 °C gave lower conversion (entries 15 and 16). The desired product **5a** was obtained in 95% yield and 86% ee in dioxane at 12 °C (entry 17).

We next examined the scope of this coupling system using α-CF_3 enones or 1,2-diones (Scheme 2). A series of enones bearing electron-withdrawing and electron-donating groups at the *para*-position of the benzene ring coupled to afford the desired products with excellent enantioselectivity (**4a–4e**, 37–81% yields, 94–98% ee). The decomposition of diarylcyclo-

This journal is © the Partner Organisations 2021

Published on 16 April 2021. Downloaded by Shaanxi Normal University on 5/27/2021 1:48:51 AM.

Table 2 Optimization of reaction conditions[a]

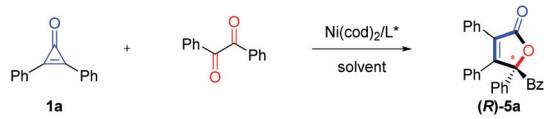

Entry	Catalyst (mol %)	L* (mol%)	Solvent	*T* (°C)	Yield (%)	ee (%)
1	$Ni(cod)_2$ (5)	**L1** (6)	Toluene	60	46	65
2	$Ni(cod)_2$ (5)	**L1** (6)	^{i}PrOH	60	21	0
3	$Ni(cod)_2$ (5)	**L1** (6)	Dioxane	60	43	53
4	$Ni(cod)_2$ (5)	**L1** (6)	THF	60	47	58
5	$Ni(cod)_2$ (5)	**L1** (6)	DCE	60	Trace	—
6	$Ni(cod)_2$ (5)	**L1** (6)	PhCl	60	44	54
7	$Ni(cod)_2$ (5)	**L1** (6)	$PhCF_3$	60	22	42
8	$Ni(cod)_2$ (5)	**L1** (6)	PhOMe	60	32	54
9	$Ni(cod)_2$ (5)	**L1** (6)	Toluene	r.t.	41	66
10	$Ni(cod)_2$ (5)	**L2** (6)	Toluene	r.t.	44	−41
11	$Ni(cod)_2$ (5)	**L3** (6)	Toluene	r.t.	48	42
12	$Ni(cod)_2$ (5)	**L4** (6)	Toluene	r.t.	49	76
13	$Ni(cod)_2$ (5)	**L5** (6)	Toluene	r.t.	85	45
14	$Ni(cod)_2$ (5)	**L6** (6)	Toluene	r.t.	77	80
15	$Ni(cod)_2$ (5)	**L6** (6)	Toluene	0	76	90
16	$Ni(cod)_2$ (5)	**L6** (6)	Toluene	−20	21	93
17	$Ni(cod)_2$ (5)	**L6** (6)	Dioxane	12	95	86

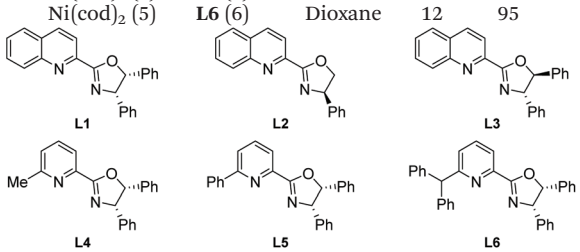

[a] Reaction conditions: **1a** (0.20 mmol), benzil (0.20 mmol), $Ni(cod)_2$ (0.01 mmol), L* (0.012 mmol), solvent (2.0 mL), 24 h under argon.

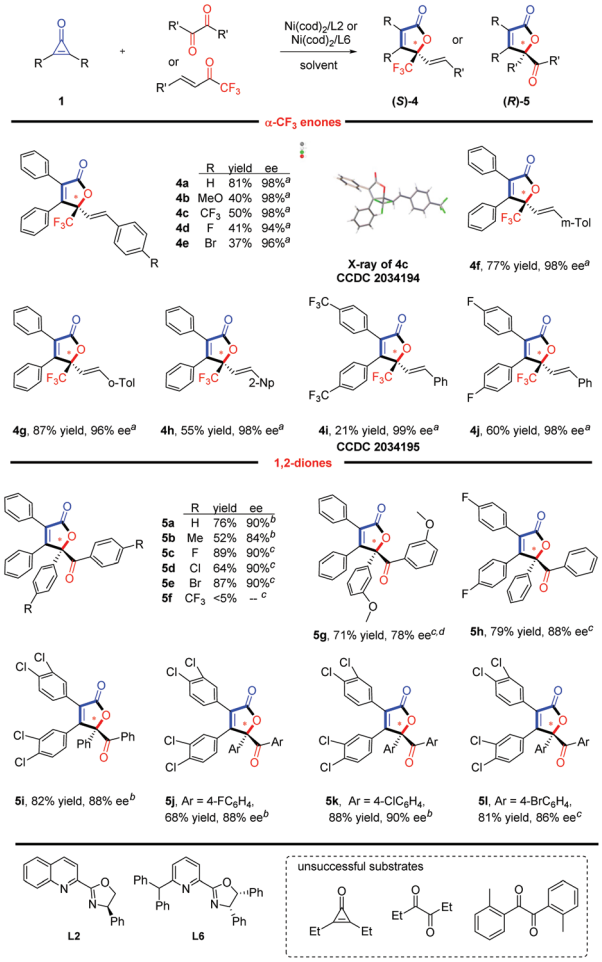

Scheme 2 Substrate scope. Reaction conditions: **1** (0.2 mmol), enone or dione (0.2 mmol), $Ni(cod)_2$ (0.01 mmol), and L* (0.012 mmol) in the solvent (2.0 mL), 24 h, isolated yield. [a] Reaction conditions A: **L2** (0.012 mmol), MeO^{t}Bu (2.0 mL), room temperature. [b] Reaction conditions B: **L6** (0.012 mmol), toluene (2.0 mL), 0 °C. [c] Reaction conditions C: **L6** (0.012 mmol), dioxane (2.0 mL), 12 °C. [d] Room temperature.

propenones occurred for some low activity systems. The reaction also worked well in the presence of a *meta*- or *ortho*-methyl group (**4f**, 77% yield, 98% ee, and **4g**, 87% yield, 96% ee). A 2-naphthyl-substituted enone also afforded the desired product **4h** in an acceptable yield with excellent enantioselectivity (98% ee). The scope of cyclopropenones was briefly examined, and diarylcyclopropenones bearing a trifluoromethyl or fluoro group were well tolerated with excellent enantioselectivity (**4i**, 21% yield, 99% ee and **4j**, 60% yield, 98% ee). The absolute configuration of **4c** and **4i** was unambiguously confirmed by X-ray crystallography. We then explored the generality of 1,2-diones as a coupling partner. A range of aryl–aryl 1,2-diketones bearing methyl, fluoro, chloro, and bromo groups at the *para* position were tolerated (**5a–5e**, 52–89% yields, 84–90% ee). The diminished efficiency of **5b** might indicate an electronic effect at the *para* position of the benzene ring. Introduction of a *meta* OMe group resulted in lower efficiency and enantioselectivity (**5g**, 71% yield and 78% ee). Several cyclopropenones were also briefly examined, and fluoro- or chloro-substituted cyclopropenones afforded the desired products in moderate yields with excellent enantioselectivities (**5h–5l**, 68–88% yields, 86–88% ee). In contrast, dialkylcyclopropenones, hexane-3,4-dione and symmetrical diarylcyclopropenones with *ortho* methyl groups all failed to undergo any coupling.

Mechanistic studies

The remarkable activity, excellent chemo- and enantioselectivity, and practicality of the coupling of enones prompted us to conduct detailed mechanistic studies to understand the unique performance. We previously briefly demonstrated that this reaction of **1a** and **2a** proceeded through an ionic reaction pathway instead of a radical reaction pathway.[8] Linear correlation between the ee of **L1** and that of **3a** suggested that only one **L1** ligand was involved in each active Ni species in the enantio-determining step.[12] Moreover, control experiments were carried out in the presence of the **L1** ligand alone to determine whether the reaction proceeds *via* organo or organometallic catalysis (Table S1, ESI†).[13] No reaction occurred in

Published on 16 April 2021. Downloaded by Shaanxi Normal University on 5/27/2021 1:48:51 AM.

the presence of the **L1** ligand and in the absence of $Ni(cod)_2$, indicating that the Ni metal is essential for the conversation. Exposure of the reaction system to air resulted in instantaneous inhibition of the reaction, while the reaction was not sensitive to water, supporting the possibility of Ni(0) species in the catalytic cycle.

Computational studies

Theoretical calculations were performed at the density functional theory level using the Gaussian 09 series of programs (B3-LYP with the standard 6-31G(d))[14] to investigate the mechanism and the origin of the enantioselectivity for this Ni (0)-catalyzed [3 + 2] annulation reaction between substrates **1a** and **2a**. In the lowest energy pathway as far as we have identified (Fig. 1), chiral ligand-bound **L1**-Ni(0) species **CP1** was set to the relative zero energy. It was found that enone **2a** has much higher affinity toward Ni(0) than cyclopropenone **1a**, and ligand exchange of enone with cyclooctadiene in **CP1** gives intermediate **CP2** with an exergonicity of 16.7 kcal mol^{-1} as a result of the stronger coordination of enone (a stronger π acceptor) than that of COD. Coordination of **1a** forms the four-coordinate Ni(0) species **CP3**, which undergoes oxidative addition of cyclopropenone *via* transition state **TS1** with a calculated free energy barrier[9] of 7.8 kcal mol^{-1}, delivering the five-coordinate, four-membered nickelacycle **CP4**. Subsequently, a rare 4,1-insertion of enone into the Ni–acyl bond was identified, which proceeds *via* the unusual six-membered ring **TS2** featuring an *endo*-type 4,1-insertion, giving the tethered allyl–Ni(II) intermediate **CP5** (*via* transition state **TS2**) with an barrier of only 14.7 kcal mol^{-1}. The C(alkenyl)–C (allyl) reductive elimination then takes place *via* transition state **TS3** with a barrier of only 14.4 kcal mol^{-1} to afford the olefin-bound Ni(0) species **CP6**. Ligand exchange with enone releases the [3 + 2] annulation product **3a** together with the active catalytic intermediate **CP2** to complete the catalytic cycle. In comparison, the alternative [3 + 4] annulation product **3a** was also considered *via* C(alkenyl)–C(distal allyl) reductive elimination of allyl–Ni(II) intermediate **CP5** *via* the transition state **TS4**. The relative energy of **TS4** is 29.8 kcal mol^{-1} higher than that of **TS3**, indicating that the [3 + 4] annulation is unlikely. DFT examination of the enantioselectivity defined by this pathway also gives the observed (*R*) enantioselectivity. On the basis of these DFT studies, **CP2** is theoretically predicted as the resting state of the catalyst, and the reaction is expected to be 0^{th} order with respect to enone **2a** and 1^{st} order for **1a**.

To understand the origin of the high enantioselectivity enabled by ligand **L1**, four diastereomeric 4,1-insertion patterns of the enone-bound transition states (**TS2-R-*endo***, **TS2-R-*exo***, **TS2-S-*endo***, and **TS2-S-*exo***) were examined.[15] The *endo* and *exo* conformations of these transition states are distinguished by the positions of allyl and phenyl olefin in the 4,1-insertion products; the conformation of **TS2** in Fig. 1 is *endo*. As shown in Fig. 2, in this stereoselectivity-determining step, the relative energy of **TS2-R-*endo*** is 15.9 kcal mol^{-1} lower than that of **TS2-R-*exo***. Analysis of the two transition states in Fig. 2 reveals that the repulsion between the phenyl group of ligand **L1** and the trifluoromethyl group of enone in **TS2-R-*exo*** raised the free energy barrier. The relative energy of **TS2-S-*endo*** is 15.1 kcal mol^{-1} lower than that of **TS2-S-*exo***. The steric repulsion between the enone substrate and the chiral center in ligand **L1** raises the energy of **TS2-S-*exo***. The relative energy of **TS2-R-*endo*** is 3.3 kcal mol^{-1} lower than that of **TS2-S-*endo***, which is in good accordance with the high (*R*) selectivity observed experimentally. Analysis of the 3D structure of **TS2-S-*exo*** shows that the steric repulsion of the trifluoromethyl group in the enone with the proximal phenyl group in the oxazoline ring of ligand **L1** contributes to the control of enantioselectivity.

As given in Fig. 1, the barrier of C–C bond cleavage of cyclopropenone is only 7.8 kcal mol^{-1}. The alternative oxidative addition of cyclopropenone onto the Ni(0) center without any ligation of the enone (three coordinate) has also been calculated. As shown in Fig. 3, ligand exchange of cyclopropenone and enone in **CP2** gives complex **CP8** with 7.3 kcal mol^{-1} endergonicity. The subsequent oxidative addition occurs *via* transition state **TS5** with an energy barrier of 24.7 kcal mol^{-1} to generate the four-membered nickelacycle **CP9**. The coordination of enone onto the Ni(II) center in **CP9** forms the five-coordinate Ni(II) intermediate **CP4** (a common intermediate in

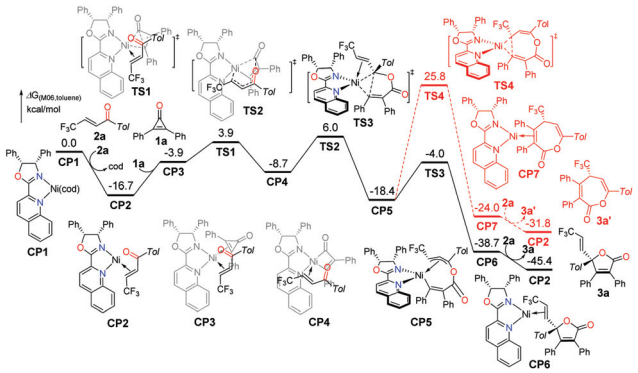

Fig. 1 Computed lowest energy pathway of the Ni(0)-catalyzed [3 + 2] annulation reaction.

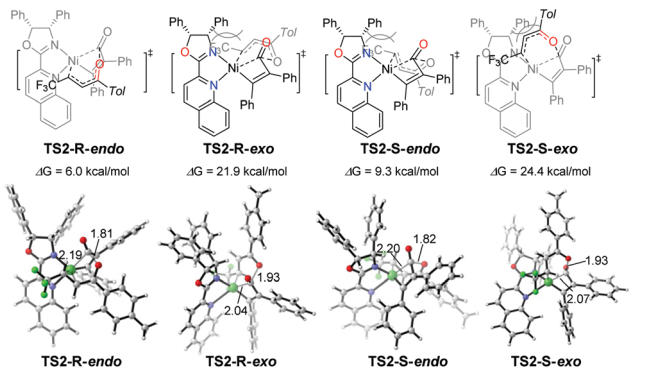

Fig. 2 DFT studies of the stereoselectivity-determining step.

This journal is © the Partner Organisations 2021

Published on 16 April 2021. Downloaded by Shaanxi Normal University on 5/27/2021 1:48:51 AM.

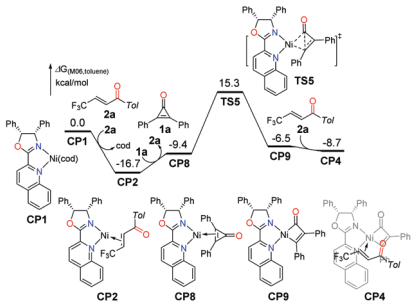

Fig. 3 Free energy profile for oxidative addition of cyclopropenone onto the Ni(0) center without ligation of enone.

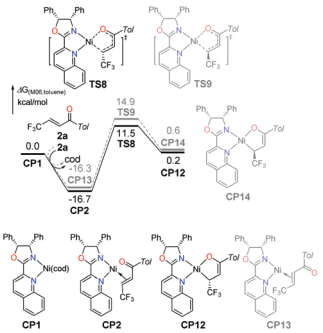

Fig. 5 Free energy profile for oxidative cyclization of enones to the Ni (0) center.

Fig. 1). The free energy of transition state **TS5** is 11.4 kcal mol^{-1} higher than that of **TS1** in Fig. 1, thus indicating that substitution of enone in **CP2** is unfavorable. The calculated results indicated that coordination of enone **1a** to the Ni(0) center would facilitate the oxidation addition process of cyclopropenone (Fig. 3). Nevertheless, this calculated pathway, if followed, corresponds to 1^{st} order kinetics of **1a** but 0^{th} order kinetics of **2a**, which is kinetically distinguishable from the kinetic profiles in Fig. 1.

The third pathway, which involves oxidative cyclization, β-C elimination, and reductive elimination, has also been considered. The calculated Gibbs energy profiles for this (bimolecular oxidative cyclization) pathway are shown in Fig. 4. Ligand exchange of enone with cyclooctadiene gives π-complex **CP2** with 16.7 kcal mol^{-1} exothermicity. The coordination of cyclopropenone to the Ni(0) center in **CP2** forms complex **CP10**. Subsequent oxidative cyclization occurs *via* transition state **TS6** with a barrier of 43.8 kcal mol^{-1} to give the seven-membered nickelacycle **CP11**. The allyl–Ni(II) intermediate **CP5** is then formed *via* β-C elimination transition state **TS7** with an overall activation free energy of 54.5 kcal mol^{-1}. The relative energy of **TS7** is 31.8 kcal mol^{-1} higher than that of **TS2**. Therefore, this pathway can be excluded (Fig. 4).

The free energy profile of an alternative simple oxidative cyclization of enone **2a** to the Ni(0) center has been calculated. As shown in Fig. 5, the π- to σ-isomerization of **CP2** affords the C–O chelating Ni(II) species **CP12** (diastereomeric mixtures) *via* transition state **TS8** with an activation barrier of 28.2 kcal mol^{-1}. The relative energy of **CP12** is 16.9 kcal mol^{-1} higher than that of **CP2**, which shows that the oxidative cyclization of enone is both thermodynamically and kinetically unfavorable.

Identification of reaction intermediates

To correlate the experimental with the DFT studies, we sought to identify the reaction intermediates. When a mixture of Ni $(cod)_2$, **L1**, and enone **2a** was stirred, the olefin complex **CP2** was obtained in a 1.8 : 1 diastereoselectivity ratio and was characterized by NMR spectroscopy (Scheme 3, eqn (1)). The diastereomeric mixture of **CP2** was also identified by ^{19}F NMR spectroscopy in a catalytic system using THF solvent, which is a less efficient solvent to allow monitoring of the reaction process (ESI†). While it is difficult to obtain the crystal structure of the isomeric complex **CP2** due to instability, we turned our attention to stabilization using achiral phosphine ligands, which also proved to be suitable ligands for this racemic [3 + 2] annulation reaction (ESI, Table S1† entry 10). By using the PPh_3 ligand, the 16-electron olefin complex **6** was isolated

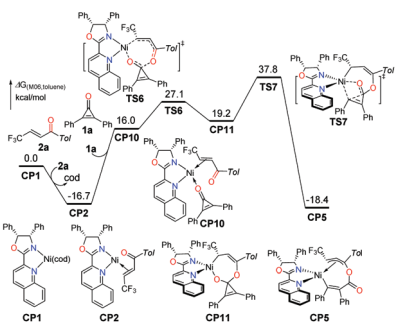

Fig. 4 Free energy profile for oxidative cyclization of enones to the Ni (0) center.

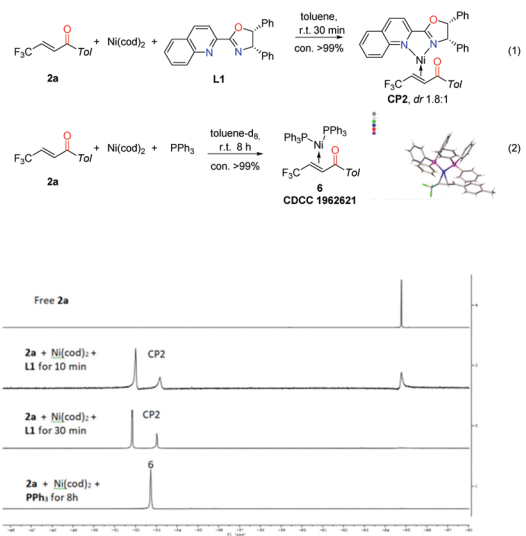

Scheme 3 The formation of the nickel-olefin intermediate and the reaction of **2a** with the nickel complex (monitored by ^{19}F NMR).

Published on 16 April 2021. Downloaded by Shaanxi Normal University on 5/27/2021 1:48:51 AM.

from a stoichiometric reaction, and the structure of **6** was unambiguously determined by X-ray crystallography.[16] Complex **6** is Y-shaped three-coordinate with two *cis* PPh_3 ligands, and no oxidative cyclization of the enone was observed even at a high temperature (Scheme 3, eqn (2)). The observation of olefin-Ni complexes in both ligand systems clearly indicates that enone **2a** is a far better ligand than COD. A further study verified that complexes **CP2** and **6** could readily catalyze the coupling of **1a** and **2a** without loss of efficiency, indicating that the olefin-Ni complex was an intermediate in the coupling reactions.[17]

Resting state study

The coupling of substrates **1a** and **2a** in the presence of Ni/PPh_3 was monitored by ^{19}F NMR, in which complex **6** was observable from the very beginning of the reaction by comparing the ^{19}F NMR spectrum of the isolated **6** with that of the reaction mixture. The concentration of **6** remained essentially constant during the reaction course using 4-(trifluoromethyl) anisole as an internal standard (Fig. 6). These results indicate that the olefin-Ni intermediate **6** is the resting state in our reaction system, and it is also in a steady state.[18]

Kinetic studies

We next conducted kinetic studies to probe the validity of our calculations. The Hammett linear correlation has been studied for the couplings of a series of *para*-electronically varied CF_3-enones **2** and **1a**, and a positive slope (ρ = +1.7) of the Hammett plot (Fig. 7a, for details see the ESI†) indicated stabilization of the negative charge in the transition state. These results are consistent with the rate-determining 4,1-insertion of enone into the Ni–acyl bond *via* six-membered ring **TS2** (Fig. 1). In addition, kinetic studies of the reaction of diphenylcyclopropenone **1a** and enone **2a** by the method of initial rates were performed. This reaction was found to be first order for cyclopropenone **1a**, indicating that **1a** is involved in the turnover-limiting step (Fig. 7b). Zero-order kinetics was observed for enone **2a** (Fig. 7c), and this observation is fully consistent with our DFT studies in Fig. 1 (with **CP2** being the resting state).

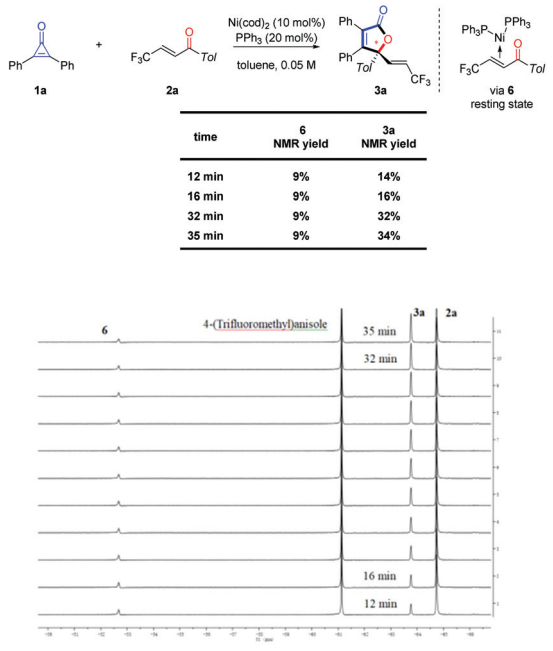

time	6 NMR yield	3a NMR yield
12 min	9%	14%
16 min	9%	16%
32 min	9%	32%
35 min	9%	34%

Fig. 6 Resting state study and ^{19}F NMR spectra of the reaction mixture.

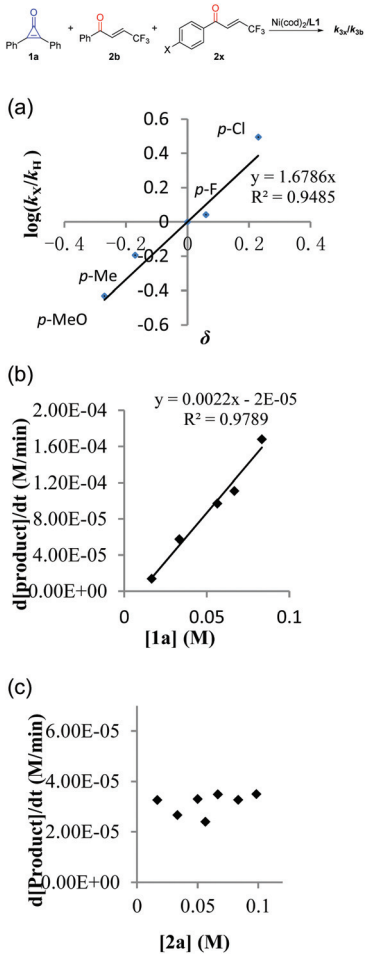

Fig. 7 Hammett equation and kinetic profile for the cyclization reactions using **L1** as the ligand. From top to bottom: (a) Hammett equation with different substituted enones **2**. (b) Plot of initial rates *versus* [**1a**]. (c) Plot of initial rates *versus* [**2a**].

Furthermore, our independent kinetic experiments using PPh_3 as a ligand were also performed, and the same observations were made. In this case, we also observed 1st order kinetics for **1a**, and zero-order kinetics for **2a**, and these results suggest that the reaction proceeded through a similar pathway using **L1** or PPh_3. The Ni(0)/PPh_3 catalyst was found to be first-order in this cyclization reaction, indicating that only one Ni center was involved in the turnover-limiting step (for details see the ESI†). Indeed, our DFT studies on the Ni/PPh_3-catalyzed system also agree well with these kinetic results.

This journal is © the Partner Organisations 2021

Published on 16 April 2021. Downloaded by Shaanxi Normal University on 5/27/2021 1:48:51 AM.

Conclusions

A comprehensive mechanistic study by combined experimental and computational approaches has been conducted to investigate the mechanism of the nickel-catalyzed enantioselective [3 + 2] annulation *via* C–C bond activation of cyclopropenones. This nickel-catalyzed system was found to be highly efficient (with a TOF up to 2208 h^{-1}). The scope of other coupling partners was further defined, and α-CF_3 enones and 1,2-diones were applicable in this asymmetric system. DFT studies revealed that the reaction is initiated by oxidative addition of diphenylcyclopropenone to olefin-bound nickel(0), followed by *endo*-type 4,1-insertion and C–C reductive elimination of a Ni (II) allyl intermediate. The olefin-Ni intermediate was found to be the resting state based on both experimental studies and DFT calculations. Computational studies also verified that coordination of the olefin unit of enone to the nickel center dramatically decreases the energy barrier of subsequent C–C oxidative addition of cyclopropenone. The rarity, high chemo- and enantioselectivity, and atom- and step-economy of this intermolecular C–C activation provide an important starting point for further development to fully exploit catalytic C–C bond activation.

Conflicts of interest

The authors declare no competing financial interest.

Acknowledgements

This work is supported by the NSFC (No. 21801067, U1804283, 21801066), the Central Plains Scholars and Scientists Studio Fund (2018002), and the project funded by the Natural Science Foundation of Henan (202300410225) and China Postdoctoral Science Foundation (2020T130176 and 2020M682306). The authors wish to acknowledge Dr Shujun Li for analysis of X-ray crystallography.

Notes and references

1 For recent reviews, see: (*a*) P. Sivaguru, Z.-K. Wang, G. Zanoni and X.-H. Bi, Cleavage of Carbon–Carbon Bonds by Radical Reactions, *Chem. Soc. Rev.*, 2019, **48**, 2615–2656; (*b*) F.-J. Song, T. Gou, B.-Q. Wang and Z.-J. Shi, Catalytic Activation of Unstrained C-C Bond Involving Organometallic Intermediates, *Chem. Soc. Rev.*, 2018, **47**, 7078–7115; (*c*) G. Fumagalli, S. Stanton and J. F. Bower, Recent Methodologies That Exploit C-C Single-Bond Cleavage of Strained Ring Systems by Transition Metal Complexes, *Chem. Rev.*, 2017, **117**, 9404–9432; (*d*) P.-H. Chen, B. A. Billett, T. Tsukamoto and G.-B. Dong, "Cut and Sew" Transformations via Transition-Metal-Catalyzed Carbon–Carbon Bond Activation, *ACS Catal.*, 2017, **7**, 1340–1360; (*e*) D.-S. Kim, W.-J. Park and C.-H. Jun, Metal–Organic Cooperative Catalysis in C–H and C–C Bond Activation, *Chem. Rev.*, 2017, **117**, 8977–9015; (*f*) M. Murakami and N. Ishida, Potential of Metal-Catalyzed C–C Single Bond Cleavage for Organic Synthesis, *J. Am. Chem. Soc.*, 2016, **138**, 13759–13769; (*g*) L. Souillart and N. Cramer, Catalytic C-C Bond Activations Via Oxidative Addition to Transition Metals, *Chem. Rev.*, 2015, **115**, 9410–9464; (*h*) F. Chen, T. Wanga and N. Jiao, Recent Advances in Transition-Metal-Catalyzed Functionalization of Unstrained Carbon–Carbon Bonds, *Chem. Rev.*, 2014, **114**, 8613–8661; (*i*) C.-H. Jun, Transition metal-catalyzed Carbon-Carbon Bond Activation, *Chem. Soc. Rev.*, 2004, **33**, 610–618; (*j*) M. Murakami and N. Chatani, *Cleavage of Carbon-Carbon Single Bonds by Transition metals*, Wiley-VCH, Weinheim, Germany, 2016; (*k*) *C–C Bond Activation*, Topics in Current Chemistry, ed. G. Dong, Springer, New York, 2014, vol. 346.

2 For recent reviews on earth-abundant metal catalysis, see: (*a*) X. Fang, P. Yu and B. Morandi, Catalytic Reversible Alkene-nitrile Interconversion Through Controllable Transfer Hydrocyanation, *Science*, 2016, **351**, 832–836; (*b*) D. Zell, Q. Bu, M. Feldt and L. Ackermann, Mild C–H/C–C Activation by Z–Selective Cobalt Catalysis, *Angew. Chem., Int. Ed.*, 2016, **55**, 7408–7412; (*c*) A. P. Dieskau, M. S. Holzwarth and B. Plietker, Fe-Catalyzed Allylic C–C-Bond Activation: Vinylcyclopropanesas Versatile a^1,a^3,d^5-Synthons in Traceless Allylic Substitutions and [3+2]-Cycloadditions, *J. Am. Chem. Soc.*, 2012, **134**, 5048–5051; (*d*) T. Kurahashi and A. de Meijere, C-C Bond Activation by Octacarbonyldicobalt: [3+1] Cocyclizations of Methylenecyclopropanes with Carbon Monoxide, *Angew. Chem., Int. Ed.*, 2005, **44**, 7881–7884. Select examples: (*e*) M. Murakami, S. Ashida and T. Matsuda, Nickel-Catalyzed Intermolecular Alkyne Insertion into Cyclobutanones, *J. Am. Chem. Soc.*, 2005, **127**, 6932–6933; (*f*) M. Murakami, H. Amii and Y. Ito, Selective Activation of Carbon-Carbon Bonds Next to a Carbonyl Group, *Nature*, 1994, **370**, 540–541; (*g*) Y. Xu, X.-T. Qi, P.-F. Zheng, C. C. Berti1, P. Liu and G.-B. Dong, Deacylative Transformations of Ketones via Aromatization-promoted C–C Bond Activation, *Nature*, 2019, **567**, 373–378; (*h*) H. Li, Y. Li, X. S. Zhang, K. Chen, X. Wang and Z. J. Shi, Pyridinyl Directed Alkenylation with Olefins via Rh(III)-catalyzed C–C Bond Cleavage of Secondary Arylmethanols, *J. Am. Chem. Soc.*, 2011, **133**, 15244–15247; (*i*) E. Ozkal, B. Cacherat and B. Morandi, Cobalt(III)-Catalyzed Functionalization of Unstrained Carbon–Carbon Bonds through *β*-Carbon Cleavage of Alcohols., *ACS Catal.*, 2015, **5**, 6458–6462; (*j*) L. Deng, L. Jin and G. Dong, Fused-Ring Formation by an . Intramolecular "Cut-and-Sew" Reaction between Cyclobutanones and Alkynes, *Angew. Chem., Int. Ed.*, 2018, **57**, 2702–2706.

3 (*a*) L. Deng, M. Chen and G.-B. Dong, Concise Synthesis of (−)-Cycloclavine and (−)-5-epi-Cycloclavine via Asymmetric C–C Activation, *J. Am. Chem. Soc.*, 2018, **140**, 9652–9658; (*b*) L. Deng, T. Xu, H.-B. Li and G.-B. Dong,

Published on 16 April 2021. Downloaded by Shaanxi Normal University on 5/27/2021 1:48:51 AM.

Enantioselective Rh-Catalyzed Carboacylation of C=N Bonds via C-C Activation of Benzocyclobutenones, *J. Am. Chem. Soc.*, 2016, **138**, 369–374; (*c*) X. Zhou and G.-B. Dong, Nickel-Catalyzed Chemo- and Enantioselective Coupling between Cyclobutanones and Allenes: vRapid Synthesis of [3.2.2] Bicycles, *Angew. Chem., Int. Ed.*, 2016, **55**, 15091–15095.

4 (*a*) L. Souillart and N. Cramer, Highly Enantioselective Rhodium(I)-Catalyzed Carbonyl Carboacylations Initiated by C–C Bond Activation, *Angew. Chem., Int. Ed.*, 2014, **53**, 9640–9644; (*b*) L. Souillart, E. Parker and N. Cramer, Highly Enantioselective Rhodium(I)-Catalyzed Activation of EnantiotopicCyclobutanone C–C Bonds, *Angew. Chem., Int. Ed.*, 2014, **53**, 3001–3005; (*c*) T. Seiser, O. A. Roth and N. Cramer, Enantioselective Synthesis of Indanols from tert-Cyclobutanols Using a Rhodium-Catalyzed C-C/C-H Activation Sequence, *Angew. Chem., Int. Ed.*, 2009, **48**, 6320–6323.

5 (*a*) N. Ishida, D. Necas, Y. Masuda and M. Murakami, Enantioselective Construction of 3-Hydroxypiperidine Scaffolds by Sequential Action of Light and Rhodium upon N-Allylglyoxylamides, *Angew. Chem., Int. Ed.*, 2015, **54**, 7418–7421; (*b*) N. Ishida, Y. Shimamoto, T. Yano and M. Murakami, 1,5-Rhodium Shift in Rearrangement of N-Arenesulfonylazetidin-3-ols into Benzosultams, *J. Am. Chem. Soc.*, 2013, **135**, 19103–19106Ni(0)-catalyzed asymmetric C–C activation: (*c*) A. Yada, S. Fujita and M. Murakami, Enantioselective Insertion of a Carbenoid Carbon into a C-C Bond to Expand Cyclobutanols to Cyclopentanols, *J. Am. Chem. Soc.*, 2014, **136**, 7217–7220; (*d*) L. Liu, N. Ishida and M. Murakami, Atom and Step-Economical Pathway to Chiral Benzobicyclo[2.2.2]octenones through Carbon-Carbon Bond Cleavage, *Angew. Chem., Int. Ed.*, 2012, **51**, 2485–2488.

6 (*a*) M. H. Shaw, N. G. McCreanor, W. G. Whittingham and J. F. Bower, Reversible C–C Bond Activation Enables Stereocontrol in Rh-Catalyzed Carbonylative Cycloadditions of Aminocyclopropanes, *J. Am. Chem. Soc.*, 2015, **137**, 463–468; (*b*) M. P. Watson and E. N. Jacobsen, Asymmetric Intramolecular Arylcyanation of Unactivated Olefins via C–CN Bond Activation, *J. Am. Chem. Soc.*, 2008, **130**, 12594–12595; (*c*) Y. Nakao, S. Ebata, A. Yada, T. Hiyama, M. Ikawa and S. Ogoshi, Intramolecular Arylcyanation of Alkenes Catalyzed by Nickel/$AlMe_2Cl$, *J. Am. Chem. Soc.*, 2008, **130**, 12874–12875.

7 Q.-S. Liu, D.-Y. Wang, Z.-J. Yang, Y.-X. Luan, J.-F. Yang, J.-F. Li, Y.-G. Pu and M.-C. Ye, Ni–Al Bimetallic Catalyzed Enantioselective Cycloaddition of Cyclopropyl Carboxamide with Alkyne, *J. Am. Chem. Soc.*, 2017, **139**, 18150–18153.

8 D.-C. Bai, Y.-J. Yu, H.-M. Guo, J.-B. Chang and X.-W. Li, Nickel(0)–Catalyzed Enantioselective [3+2] Annulation of Cyclopropenones and α,β–Unsaturated Ketones/Imines, *Angew. Chem., Int. Ed.*, 2020, **59**, 2740–2744.

9 (*a*) B. Mao, M. Fañanás-Mastra and B. L. Feringa, Catalytic Asymmetric Synthesis of Butenolides and Butyrolactones, *Chem. Rev.*, 2017, **117**, 10502–10566; (*b*) J. Ji, L. Lin, Q. Tang, T. Kang, X. Liu and X. Feng, Highly Efficient Asymmetric Synthesis of Chiral γ-Alkenyl Butenolides Catalyzed by Chiral *N,N′*-Dioxide–Scandium(III) Complexes, *ACS Catal.*, 2017, **7**, 3763–3767.

10 (*a*) T. Hiyama, K. Kanie, T. Kusumoto, Y. Morizawa and M. Shimizu, *Organofluorine Compounds: Chemistry and Application*, Springer, Berlin, 2000; (*b*) P. Kirsch, *Modern Fluoroorganic Chemistry: Synthesis Reactivity, Applications*, Wiley-VCH, Weinheim, 2004; (*c*) S. Purser, P. R. Moore, S. Swallow and V. Gouverneur, Fluorine in Medicinal Chemistry, *Chem. Soc. Rev.*, 2008, **37**, 320–330.

11 (*a*) G. Choi, H. E. Kim, S. Hwang, H. Jang and W. J. Chung, Phosphorus(III)-Mediated, Tandem Deoxygenative Geminal Chlorofluorination of 1,2-Diketones, *Org. Lett.*, 2020, **22**, 4190–4195; (*b*) T.-S. Zhu, S.-S. Jin and M.-H. Xu, Rhodium–Catalyzed, Highly Enantioselective 1, 2–Addition of Aryl Boronic Acids to α–Ketoesters and α–Diketones Using Simple, Chiral Sulfur–Olefin Ligands, *Angew. Chem., Int. Ed.*, 2012, **51**, 780–783.

12 (*a*) M. Kalek and G. C. Fu, Caution in the Use of Nonlinear Effects as a Mechanistic Tool for Catalytic Enantioconvergent Reactions: Intrinsic Negative Nonlinear Effects in the Absence of Higher-Order Species, *J. Am. Chem. Soc.*, 2017, **139**, 4225–4229; (*b*) C. Girard and H. B. Kagan, Nonlinear Effects in Asymmetric Synthesis and Stereoselective Reactions: Ten Years of Investigation, *Angew. Chem., Int. Ed.*, 1998, **37**, 2922–2959; (*c*) D. Guillaneux, S.-H. Zhao, O. Samuel, D. Rainford and H. B. Kagan, Nonlinear Effects in Asymmetric Catalysis, *J. Am. Chem. Soc.*, 1994, **116**, 9430–9439.

13 (*a*) J. Xu, J. Cao, C. Fang, T. Lu and D. Du, Organocatalytic C–C bond activation of cyclopropenones for ring-opening formal [3+2] cycloaddition with isatins, *Org. Chem. Front.*, 2017, **4**, 560–564; (*b*) Y. Wei, W. Zhao, Y. Yang, Z. Zhang and M. Shi, Allenic Esters from Cyclopropenones by Lewis Base Catalysis: Substrate Scope, the Asymmetric Variant from the Dynamic Kinetic Asymmetric Transformation, and Mechanistic Studies, *ChemCatChem*, 2015, **7**, 3340–3349; (*c*) Y. Yang, Z. Zhang, X. Zhang, D. Wang, Y. Wei and M. Shi, Lewis base-catalyzed reactions of cycloprvopenones: novel synthesis of mono- or multi-substituted allenic esters, *Chem. Commun.*, 2014, **50**, 115–117; (*d*) X. Li, C. Han, H. Yao and A. Lin, Organocatalyzed [3+2] Annulation of Cyclopropenones and β-Ketoesters: An Approach to Substituted Butenolides with a Quaternary Center, *Org. Lett.*, 2017, **19**, 778–781; (*e*) P. A. Wender, T. J. Paxton and T. J. Williams, Cyclopentadienone Synthesis by Rhodium(I)-Catalyzed [3+2] Cycloaddition Reactions of Cyclopropenones and Alkynes, *J. Am. Chem. Soc.*, 2006, **128**, 14814–14815; (*f*) A. Baba, Y. Ohshiro and T. Agawa, Reactions of Diphenylcyclopropenone With N-sulfinylamines in the Presence of Nickel Tetracarbonyl, *Chem. Lett.*, 1976, **5**, 11–12; (*g*) A. Baba, Y. Ohshiro and T. Agawa, Reactions Of Diphenylcyclopenone with ketene

 This journal is © the Partner Organisations 2021

Published on 16 April 2021. Downloaded by Shaanxi Normal University on 5/27/2021 1:48:51 AM.

in the Presence of Nickel Tetracarbonyl, *J. Organomet. Chem.*, 1976, **110**, 121–127.

14 (*a*) A. D. Becke, Density–Functional Thermochemistry. III. The Role of Exact Exchange, *J. Chem. Phys.*, 1993, **98**, 5648–5652; (*b*) C. Lee, W. Yang and R. G. Parr, *Phys. Rev. B: Condens. Matter Mater. Phys.*, 1988, **37**, 785–789.

15 (*a*) L. Tao, X.-Y. Guo, J. Li, R.-L. Li, Z.-Y. Lin and W.-X. Zhao, Rhodium-Catalyzed Deoxygenation and Borylation of Ketones: A Combined Experimental and Theoretical Investigation, *J. Am. Chem. Soc.*, 2020, **142**, 18118–18127; (*b*) X. Zhang, Mechanistic Study of the Nickel-Catalyzed α,β-Coupling of Saturated Ketones, *ACS Catal.*, 2018, **8**, 1740–1747; (*c*) S. Ogoshi, T. Haba and M. Ohashi, Nickel-Catalyzed Direct Conjugate Addition of Simple Alkenes to Enones, *J. Am. Chem. Soc.*, 2009, **131**, 10350–10351; (*d*) J. D. Siebe and J. P. Morken, Asymmetric Ni-Catalyzed Conjugate Allylation of Activated Enones, *J. Am. Chem. Soc.*, 2008, **130**, 4978–4983; (*e*) J. d. Pozo, E. Gioria and P. Espinet, Olefin Insertivon Versus Cross-Coupling in trans-[Pd(Ar)X($AsPh_3$)$_2$] Complexes (X=I, F, CF_3) Treated with a Phosphine-EWOlefin Ligand to Induce Ar–X Coupling, *Organometallics*, 2017, **36**, 2884–2890.

16 Select examples of 16-electron olefin-Ni complexes: (*a*) I. Jevtovikj, S. Manzini, M. Hanauer, F. Romingerc and T. Schaub, Investigations on the catalytic carboxylation of olefins with CO_2 towards α,β-unsaturated carboxylic acid salts: characterization of intermediates and ligands as well as substrate effects, *Dalton Trans.*, 2015, **44**, 11083–11094; (*b*) J. D. Sieber and J. P. Morken, Asymmetric Ni-Catalyzevd Conjugate Allylation of Activated Enones, *J. Am. Chem. Soc.*, 2008, **130**, 4978–4983; (*c*) K. R. Pórschke, Mono- and bis (ethyne)nickel(0) complexes, *J. Am. Chem. Soc.*, 1989, **111**, 5691–5699.

17 Select examples of three-coordinate nickel complexes: (*a*) J. Cornella, E. Gomez-Bengoa and R. Martin, Combined Experimental and Theoretical Study on the Reductive Cleavage of Inert C–O Bonds with Silanes: Ruling out a Classical Ni(0)/Ni(II) Catalytic Couple and Evidence for Ni(I) Intermediates, *J. Am. Chem. Soc.*, 2013, **135**, 1997–2009; (*b*) B. Horn, C. Limberg, C. Herwig and B. Braun, Nickel(I)-mediated transformations of carbon dioxide in closed synthetic cycles: reductive cleavage and coupling of CO_2 generating $Ni^{I}CO$, $Ni^{II}CO_3$and $Ni^{II}C_2O_4$NiIIentities, *Chem. Commun.*, 2013, **49**, 10923–10925; (*c*) S. Pfirrmann, C. Limberg, C. Herwig, C. Knispel, B. Braun, E. Bill and R. Stösser, Reduced β-Diketiminato-Ligated Ni_3H_4 Unit Catalyzing H/D Exchange, *J. Am. Chem. Soc.*, 2010, **132**, 13684–13691; (*d*) N. A. Eckert, A. Dinescu, T. R. Cundari and P. L. Holland, A T-Shaped Three-Coordinate Nickel(I) Carbonyl Complex and the Geometric Preferences of Three-Coordinate d^9 Complexes, *Inorg. Chem.*, 2005, **44**, 7702–7704.

18 (*a*) J. Zhu, P. H. Chen, G. Lu, P. Liu and G. B. Dong, Ruthenium-Catalyzed Reductive Cleavage of Unstrained Aryl–Aryl Bonds: Reaction Development and Mechanistic Study, *J. Am. Chem. Soc.*, 2019, **141**, 18630–18640; (*b*) E. Alvaro and J. F. Hartwig, Resting State and Elementary Steps of the Coupling of Aryl Halides with Thiols Catalyzed by Alkylbisphosphine Complexes of Palladium, *J. Am. Chem. Soc.*, 2009, **131**, 7858–7868.